SEISMIC AVOaz INVERSION IN LOW-LOSS VISCOELASTIC ORTHORHOMBIC MEDIUM

ZIJIAN GE[1], SHULIN PAN[1], JINGYE LI[2], JIANBO HUANG[3], HAORAN LUO[4] and JIANG HE[1]

[1] *School of Geosciences and Technology, Southwest Petroleum University, Chengdu 610500, P.R. China. shulinpan@swpu.edu.cn*
[2] *State Key Laboratory of Petroleum Resources and Prospecting, China University of Petroleum, Beijing 102249, P.R. China.*
[3] *Engineering Technology Research Institute, Xinjiang Oilfield Company, Karamay 830011, P.R. China.*
[4] *Shale Gas Research Institute, Petro China Southwest Oil & Gasfield Company, Chengdu 610051, P.R. China.*

(Received August 28, 2020; Revised version accepted September 19, 2021)

ABSTRACT

Ge, Z.J., Pan, S.L., Li, J.Y., Huang, J.B., Luo, H.R. and He, J., 2001. Seismic AVOaz inversion in low-loss viscoelastic orthorhombic medium. *Journal of Seismic Exploration*, 30: 545-560.

The real shale reservoirs are conventionally equivalent to the orthorhombic medium, which contains a large number of high angle fractures and strong horizontal bedding properties. The attenuation effect due to frequency-dependent absorption and wave-front divergence can reveal the location of oil and gas reservoirs. Weak anisotropy parameters (WA) and fracture compliances provide additional brittleness and fluid type information in the description of orthorhombic anisotropy (OA). In this paper, the complex WA parameters and fracture compliances associated with inverse quality factors are introduced into the reflection coefficient of OA medium. After a series of simplifications and derivations, a linear reflection coefficient formula with attenuation term expressed by integrated attenuation factor is available. Integrated attenuation factor refers to the product of inverse quality factors of dissipative background and fracture. Finally, WA parameters, fracture compliances and integrated inverse quality factors can be estimated by amplitude versus offset and azimuth (AVOA) inversion based on Bayesian frame. When applied to synthetic multi-azimuth angle gathers with signal-to-noise ratio (SNR) of 2, the proposed method shows reliable stability and accuracy.

KEY WORDS: seismic anisotropy, attenuation, inversion theory, orthorhombic medium.

0963-0651/21/$5.00

INTRODUCTION

In unconventional oil and gas resources, shale gas has great potential as an alternative energy for conventional oil and gas resources. In sedimentary basins, Shale rock commonly has horizontal bedding structure and high angle fracture-developed properties due to the rich brittle minerals. Therefore, the combination of vertical transverse isotropic (VTI) background and fracture-induced horizontal transversely isotropic (HTI) symmetry yields the orthorhombic anisotropy (OA) in shale reservoir.

The linear slip theory describes how to use fracture normal and tangential compliances or weaknesses to characterize the linear relationship between displacement difference and traction vector of fracture face (Schoenberg and Sayers, 1995). Hsu and Schoenberg (1993) established the relationship between fracture compliances and weaknesses. The compliance or stiffness matrix contains the information of fracture properties. Assuming that fracture is a circular-shaped model, the compliance matrix defined by Sayers (2009), Far et al. (2013) and Ge et al. (2020) embodies the density, area, strike and particular compliances of fractures. However, the stiffness matrix involving normal and tangential fracture weaknesses implies density, aspect ratio, and fluid of fractures (Bakulin et al., 2000).

The seismic wave is affected by frequency-dependent absorption and wave-front diffusion during underground propagation, which causes instability in amplitude and frequency of seismic wave with traveltime (Pointer et al., 2000). Some simple methods can be used to compensate wave-front diffusion. The frequency-dependent attenuation, referred to as the inverse quality factor Q^{-1}, involves mineral composition, rock skeleton and fluid type in rocks (Chapman et al., 2002; Chapman et al., 2006). Many published papers have discussed and proposed rock physics attenuating models related to P- and S-wave velocities, moduli and inverse quality factors in viscoelastic rocks (Biot, 1962; Dvorkin and Nur, 1993; Dvorkin et al., 1995; Aki and Richards, 2002; Dvorkin and Mavko, 2006; Mavko et al., 2009). In fractured rocks, the inverse quality factors are not only affected by the intrinsic viscoelasticity of background rock, but also by the viscous fluid in pores or fractures and liquids migration between communicating pores or fractures. Hudson et al. (1996) develop an effective fractured attenuating models by introducing dynamic properties of fluid and its flow. Pointer et al. (2000) analyse the influence of fracture arrangement on seismic wave velocity and attenuation properties in different cases of fluid movement mechanisms. Chapman (2003) establish a fractured rock model considering both microcrack and long fractures, which can reflect frequency-dependent anisotropy and attenuation in seismic frequency band. In viscoelastic HTI media, Chichinina et al. (2006) define the expression of inverse quality factor and built the relationship between Q-dependent Thomsen parameters and fracture weaknesses. Assuming weak anisotropy and low attenuation, Zhu and Tsvankin (2006) define Thomsen-type weak anisotropy parameter related to attenuation for viscoelastic transversely isotropic (TI) media. Moradi and Innanen (2017) derive perturbations of VTI stiffness tensor in the case of weak anisotropy and low-loss attenuation and construct scattering formula based Born approximation for (amplitude variation with offset) AVO and (full waveform inversion) FWI.

Many papers have been published about prediction of attenuation properties from seismic amplitude reflection or seismic elastic impedance (Chen et al., 2018; Chen and Innanen, 2018). Bayesian and ISTA algorithm can be used to solve the inversion equation (Ge et al., 2018; Pan et al., 2019, 2020a,b). The current viscoelastic amplitude versus offset and azimuth (AVOA) methods are mainly aimed at isotropic or HTI media. Therefore, the prediction of attenuation properties of fractured rocks with VTI background of sedimentary horizontal bedding needs to be studied.

In this paper, we first assume that the orthotropic medium has WA and weak attenuation. In this case, we first derive the expression of complex fracture compliances related to attenuation. Combining complex VTI stiffness coefficients and complex fracture compliance matrix, we then calculate complex generalized WA parameters from the stiffness coefficients of viscoelastic OA media. Following Sayers (2009) and Far et al. (2013), we derive a general reflection coefficient formula linearly related to complex fracture compliance tensors. By rewriting this general reflection coefficient and some simplification, we obtain a linearized reflection coefficient referred to WA parameters, specific compliances and new inverse quality factors. Finally, we create a linear AVOA inversion method with Bayesian framework. The stability and accuracy of new method are analysed by numerical simulation of noisy synthetic data.

THEORY AND METHODS

The stiffness coefficients for VTI-viscoelastic media

The complex stiffness coefficients $\widetilde{C_{mn}} = C_{mn} + iC_{mn}^{\mathrm{Im}}$ of viscoelastic media can be written as real part C_{mn} associated with elastic and anisotropic properties plus imaginary part C_{mn}^{Im} due to attenuation:

$$\widetilde{C_{mn}} = C_{mn} + iC_{mn}^{\mathrm{Im}}, \tag{1}$$

where, inverse quality factors are defined as $Q_{mn}^{-1} = C_{mn}^{\mathrm{Im}} / C_{mn}$.

The stiffness coefficients of VTI-viscoelastic media can be written in terms of P- and S-wave moduli of isotropic background M, μ, WA parameters $\varepsilon, \gamma, \delta$ and P- and S-wave inverse quality factors Q_P^{-1}, Q_S^{-1} (Moradi and Innanen, 2017):

$$\widetilde{C_{33}} = M\left(1 + iQ_P^{-1}\right) \quad , \tag{2}$$
$$\widetilde{C_{55}} = \mu\left(1 + iQ_S^{-1}\right)$$
$$\widetilde{C_{11}} = M\left(1 + 2\varepsilon\right) + iQ_P^{-1}M\left(1 + 2\varepsilon + \varepsilon_Q\right)$$
$$\widetilde{C_{66}} = \mu\left(1 + 2\gamma\right) + iQ_S^{-1}\mu\left(1 + 2\gamma + \gamma_Q\right)$$
$$\widetilde{C_{13}} = M\left(1 + \delta\right) - 2\mu + iQ_P^{-1}M\left(1 + \delta + \delta_Q\right) - 2iQ_S^{-1}\mu$$

where, Q-dependent WA parameters $\varepsilon_Q, \gamma_Q, \delta_Q$ are assumed to be much smaller than 1 (Zhu and Tsvankin, 2006).

The complex normal and tangential fracture compliances

For fractured media with isotropic background, the relationship between fracture weaknesses and compliances is expressed by Hsu and Schoenberg (1993) as:

$$\delta_N = \frac{MB_N}{1+MB_N}, \tag{3}$$
$$\delta_T = \frac{\mu B_T}{1+\mu B_T}$$

where δ_N and δ_T denote normal and tangential weaknesses, respectively. B_N and B_T are normal and tangential compliances, respectively. Considering the B_N viscoelastic properties of background medium and the attenuation caused by fractures, the real elastic parameters, real fracture compliances and weaknesses are changed into complex type, so that complex compliances can be rewritten as,

$$\widetilde{B_N} = \frac{\widetilde{\delta_N}}{\widetilde{M}\left(1-\widetilde{\delta_N}\right)} \quad , \tag{4}$$
$$\widetilde{B_T} = \frac{\widetilde{\delta_T}}{\tilde{\mu}\left(1-\widetilde{\delta_T}\right)}$$

where $\widetilde{M}$ and $\widetilde{\mu}$ are the complex P- and S-wave moduli of viscoelastic isotropic background. Based on complex P- and S-wave velocity, simplified complex P- and S-wave moduli can be derived as follows in the case of weak attenuation (Chen and Innanen, 2018):

$$\begin{aligned} \widetilde{M} &\approx M + iMQ_p^{-1} \\ \widetilde{\mu} &= \mu + i\mu Q_s^{-1} \end{aligned} \quad . \tag{5}$$

The complex weaknesses $\widetilde{\delta_N}, \widetilde{\delta_T}$ of lossy HTI medium are defined as (Chichinina et al., 2006):

$$\begin{aligned} \widetilde{\delta}_N &= \delta_N - i(1-\delta_N)Q_N^{-1} \\ \widetilde{\delta}_T &= \delta_T - i(1-\delta_T)Q_T^{-1} \end{aligned} \quad , \tag{6}$$

where Q_N^{-1} and Q_T^{-1} are normal and tangential inverse quality factors induced by fluid and fluid movement between connected fractures. In the seismic frequency band (about 1-100 Hz), the tangential attenuation Q_T^{-1} is close to zero, and neglecting the imaginary part of complex tangential weakness $\widetilde{\delta}_T$ makes it approximately equal to real type (Pointer et al., 2000).

In the case of small fracture weaknesses $\delta_N, \delta_T = 1$ and low loss $Q_P^{-1}, Q_S^{-1}, Q_N^{-1} = 1$, complex compliances involving Q_N^{-1} and Q_S^{-1} can be derived by substituting eqs. (5) and (6) into eq. (4):

$$\begin{aligned} \widetilde{B}_N &= \frac{\delta_N - Q_p^{-1}Q_N^{-1}}{M(1-\delta_N)} - i\left(\frac{1}{M(1-\delta_N)}Q_N^{-1}\right) \approx \frac{\delta_N}{M(1-\delta_N)} - i\left(\frac{1}{M}Q_N^{-1}\right) \approx B_N - i\left(\frac{1}{M}Q_N^{-1}\right) \\ \widetilde{B}_T &= B_T - iB_T Q_s^{-1} \end{aligned} \quad . \tag{7}$$

In simplification, the high-order terms of Q_P^{-1}, Q_S^{-1} and Q_N^{-1}, and the term proportional to $\delta_N Q_P^{-1}$ are neglected.

The Viscoelastic stiffness matrix of orthorhombic medium

According to the scattering theorem, the total compliance of fractured solid rock can be taken as the superposition of background compliance S^0 and disturbance compliance ΔS caused by fractures (Hill, 1963; Sayers and Kachanov, 1995):

$$S_{ijkl} = S^0_{ijkl} + \Delta S_{ijkl} \quad . \tag{8}$$

In order to introduce attenuation knowledge of background medium and fractures, the complex perturbation term of rock compliance $\tilde{\Delta S}$, second-order $\tilde{\alpha}_{ij}$ and fourth-order compliance tensors $\tilde{\beta}_{ijkl}$, specific tangential $\tilde{B}_T$ and normal compliances $\tilde{B}_N$ and stiffness matrix of VTI-viscoelastic background $\tilde{C}_0$ are used to replace the corresponding parameters in the formula for elastic OA medium.

The compliance matrix of OA medium with VTI background (Fig.1) are expressed as (Far et al., 2013):

$$\tilde{\alpha}_{ij} = N_V \bar{A} \widetilde{B_T} \begin{bmatrix} \sin^2\varphi & \cos\varphi\sin\varphi & 0 \\ \cos\varphi\sin\varphi & \cos^2\varphi & 0 \\ 0 & 0 & 0 \end{bmatrix},$$

$$\tilde{\beta}_{ijkl} = N_V \bar{A} \left(\widetilde{B_N} - \widetilde{B_T}\right) \begin{bmatrix} \sin^4\varphi & \sin^2\varphi\cos^2\varphi & 0 & 0 & 0 & 2\sin^3\varphi\cos\varphi \\ \sin^2\varphi\cos^2\varphi & \cos^4\varphi & 0 & 0 & 0 & 2\sin\varphi\cos^3\varphi \\ 0 & 0 & 0 & 0 & 0 & 0 \\ 0 & 0 & 0 & 0 & 0 & 0 \\ 0 & 0 & 0 & 0 & 0 & 0 \\ 2\sin^3\varphi\cos\varphi & 2\sin\varphi\cos^3\varphi & 0 & 0 & 0 & 4\sin^2\varphi\cos^2\varphi \end{bmatrix} \tag{9}$$

where N_v represents fracture density defined as fracture number per unit volume, $\overline{A}$ is the average area of a single group of fractures, and denotes φ azimuthal angle between the fracture orientation and the reference axis.

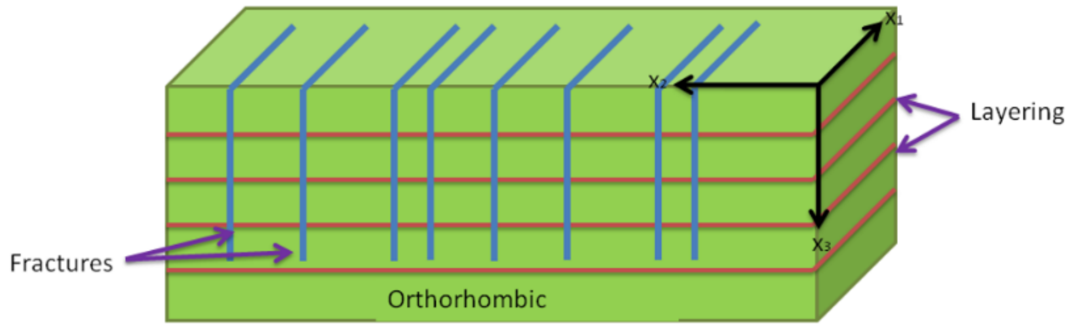

Fig. 1. Orthorhombic symmetry formed by 1 group of fractures embedded in VTI background.

Compared with the compliance matrix, stiffness matrix is more closely related to the elastic or anisotropic parameters of rock. Therefore, the simple mathematical matrix transformation is used to transform the compliance matrix into the stiffness matrix to facilitate further seismic forward and inversion research. Assuming that the disturbance compliance $\Delta\tilde{S}$ is small, the relationship between rock stiffness matrix $\tilde{C}$ and background stiffness matrix $\tilde{C}_0$ can be written by (Sayers, 2009):

$$\tilde{C} = \tilde{C}_0 - \tilde{C}_0 \Delta\tilde{S}\tilde{C}_0 \quad , \tag{10}$$

where the disturbance compliance matrix with arbitrary symmetry is constructed as:

$$\Delta\tilde{S} = \begin{bmatrix} \tilde{\alpha}_{11} + \tilde{\beta}_{1111} & \tilde{\beta}_{1122} & 0 & 0 & 0 & \tilde{\alpha}_{12} + 2\tilde{\beta}_{1112} \\ \tilde{\beta}_{1122} & \tilde{\alpha}_{11} + \tilde{\beta}_{1111} & 0 & 0 & 0 & \tilde{\alpha}_{12} + 2\tilde{\beta}_{1222} \\ 0 & 0 & 0 & 0 & 0 & 0 \\ 0 & 0 & 0 & \tilde{\alpha}_{22} & \tilde{\alpha}_{12} & 0 \\ 0 & 0 & 0 & \tilde{\alpha}_{12} & \tilde{\alpha}_{11} & 0 \\ \tilde{\alpha}_{12} + 2\tilde{\beta}_{1112} & \tilde{\alpha}_{12} + 2\tilde{\beta}_{1222} & 0 & 0 & 0 & \tilde{\alpha}_{11} + \tilde{\alpha}_{22} + 4\tilde{\beta}_{1122} \end{bmatrix} \tag{11}$$

The linearized reflection coefficient of orthorhombic medium

In this article, the PP-wave reflection coefficient of WA orthorhombic media proposed by Pšencík and Martins (2001) is used as basic forward equation for derivation:

$$R_{pp}\left(\theta,\phi\right)=R_{PP}^{iso}\left(\theta\right)+\frac{1}{2}\Delta\varepsilon_z+\frac{1}{2}\begin{bmatrix}\left(\Delta\delta_x-8\frac{\bar{V}_s^2}{\bar{V}_p^2}\Delta\gamma_x\right)\cos^2\phi+\\ \left(\Delta\delta_y-8\frac{\bar{V}_s^2}{\bar{V}_p^2}\Delta\gamma_y\right)\sin^2\phi+\\ 2\left(\Delta X_z-4\frac{\bar{V}_s^2}{\bar{V}_p^2}\Delta\varepsilon_{45}\right)\cos\phi\sin\phi-\Delta\varepsilon_z\end{bmatrix}\sin^2\theta+,$$

$$\frac{1}{2}\left[\Delta\varepsilon_x\cos^4\phi+\Delta\varepsilon_y\sin^4\phi+\Delta\delta_z\cos^2\phi\sin^2\phi+2\left(\Delta\varepsilon_{16}\cos^2\phi+\Delta\varepsilon_{26}\sin^2\phi\right)\cos\phi\sin\phi\right]\sin^2\theta\tan^2\theta \quad (12)$$

where θ denotes the incident angle, ϕ denotes the azimuthal angle, $R_{PP}^{iso}\left(\theta\right)$ represents the isotropic reflection coefficient independent of any anisotropic feature. The short line on the letters, such as $\bar{V}_p$, denotes the average P-wave velocity of upper and lower layers. The symbol Δ, such as $\Delta\varepsilon_z$, denotes the difference of generalized WA parameter ε_z between upper and lower layers. Each generalized WA parameters are expressed as

$$\delta_x=\frac{A_{13}+2A_{55}-V_p^2}{V_p^2},\delta_y=\frac{A_{23}+2A_{44}-V_p^2}{V_p^2},\delta_z=\frac{A_{12}+2A_{66}-V_p^2}{V_p^2},$$
$$X_z=\frac{A_{36}+2A_{45}}{V_p^2},\varepsilon_{16}=\frac{A_{16}}{V_p^2},\varepsilon_{26}=\frac{A_{26}}{V_p^2},\varepsilon_{45}=\frac{A_{45}}{V_p^2},\varepsilon_x=\frac{A_{11}-V_p^2}{2V_p^2},$$
$$\varepsilon_y=\frac{A_{22}-V_p^2}{2V_p^2},\varepsilon_z=\frac{A_{33}-V_p^2}{2V_p^2},\gamma_x=\frac{A_{55}-V_s^2}{2V_s^2},\gamma_y=\frac{A_{44}-V_s^2}{2V_s^2} \quad (13)$$

where the P- and S-wave velocities V_p,V_s of background isotropic medium are assumed to be known in the following derivation and $A_{ij}=\frac{C_{ij}}{\rho}$.

For Viscoelastic OA medium, we combine eqs. (2), (10) and (11) and replace A_{ij} in eq. (13), which yields the complex generalized WA parameters related to WA parameters, background attenuative factors and complex compliance tensors. Assuming that small compliance tensors $|\widetilde{\alpha}|,|\widetilde{\beta}| << 1$, weak WA parameters $|\varepsilon|,|\gamma|,|\delta| << 1$, low-loss Q-dependent WA parameters $|\varepsilon_Q|,|\gamma_Q|,|\delta_Q| << 1$ and low-loss inverse quality factors of background $Q_P^{-1}, Q_S^{-1} << 1$, we neglect high-order terms of WA parameters, Q-dependent WA parameters and inverse quality factors of background, and the product terms of any two of the four parameters (compliance tensors, WA parameters, Q-dependent WA parameters and background attenuative factors).

By introducing the generalized WA parameters into eq. (12), we can obtain the expression of reflection coefficient linearizing the model parameters:

$$R_{pp}(\theta,\phi) = R_{PP}^{iso}(\theta) + R_{PP}^{adi}(\theta) + F_1(\theta)\delta + F_2(\theta)\varepsilon + \widetilde{F_3}(\theta,\phi)\widetilde{\alpha}_{11} + \widetilde{F_4}(\theta,\phi)\widetilde{\alpha}_{12} + \widetilde{F_5}(\theta,\phi)\widetilde{\alpha}_{22} + \widetilde{F_6}(\theta,\phi)\widetilde{\beta}_{1111} + \widetilde{F_7}(\theta,\phi)\widetilde{\beta}_{1112} + \widetilde{F_8}(\theta,\phi)\widetilde{\beta}_{1122} + \widetilde{F_9}(\theta,\phi)\widetilde{\beta}_{1222} + \widetilde{F_{10}}(\theta,\phi)\widetilde{\beta}_{2222},$$

(14)

F is the sensitivity matrix. For details, please refer to the formula (25) in the paper published by Far et al. (2013).

Fracture compliance tensors are integrated embodiment of many fracture property parameters (such as density, area and strike of fracture). Reservoir physicists pay more attention to the physical parameters directly related to fracture. Therefore, it is difficult to directly characterize fractured reservoirs only by inversion of compliance tensor. Furthermore, taking 8 unknown parameters as inversion targets greatly reduces the stability and accuracy of the results. Considering the importance of specific compliances in characterization of fracture and attenuative factors in prediction of fluid, the reflection coefficient for directly estimating specific compliances and attenuative factors is derived under the assumption that the fracture density, area and azimuth has been computed accurately before inversion:

$$R_{pp}(\theta,\phi) = R_{PP}^{iso}(\theta) + R_{PP}^{adi}(\theta) + P_1(\theta)\delta + P_2(\theta)\varepsilon + P_3(\theta,\phi)B_T + P_4(\theta,\phi)B_N + P_5(\theta,\phi)Q_{PN}^{-1} + P_6(\theta,\phi)Q_{SN}^{-1}, \quad (15)$$

where $Q_{PN}^{-1} = Q_P^{-1} Q_N^{-1}$ and $Q_{SN}^{-1} = Q_S^{-1} Q_N^{-1}$ are the integrated P- and S-wave inverse quality factors, respectively. ***P*** is the sensitivity of WA parameters, specific compliance and comprehensive attenuation factor. Assuming small specific compliances $B_N, B_T = 1$ and low-loss inverse quality factors of background, we neglect the product terms of any two of the four parameters (B_N, B_T, Q_P^{-1}, Q_S^{-1}).

EXAMPLES AND RESULTS

A two-step inversion strategy is adopted to estimate the azimuth-independent WA terms and the azimuth-dependent fracture attenuation terms. In this article, synthetic AVOA data will be used to verify reliability of proposed method in inversion of WA parameters, specific compliances and attenuative factors. The geological model used in the experiment has viscoelastic orthorhombic symmetry. It is assumed that fracture azimuths are 70°. In fact, it is difficult to obtain two important property parameters (fracture aperture and radius) accurately in micro scale. Under different lithology or compaction, the fracture aperture can vary in the order of millimeter to centimeter. In general, the fracture aperture decreases with burial depth. Because of the different stress and strain conditions in the field, the fracture aperture information of the whole work area cannot be completely and accurately obtained from outcrop or core data. The results by Ge et al. (2020) show that fracture aperture has a significant influence on the estimation of fracture density. Acceptably, fracture aperture will not change greatly within the reservoir depth (Worthington, 2008). Similarly, fracture radius measured from logging or core is not credible because fracture cannot extend indefinitely in the stratum and multiple short fractures may be welded together to form long fractures at the end points (Worthington, 2008). In order to deal with this problem, we use the average value to equivalent the fracture aperture and radius in the study area. Based on the empirical data of seismic anisotropy interpretation researchers, this paper assumes that average fracture aperture and radius are 1 mm and 10 m, respectively. Thus, the average fracture area is 0.02 m^2. We have constructed specific compliances and integrated attenuative factors curves with variation at depth, as displayed in Fig. 2.

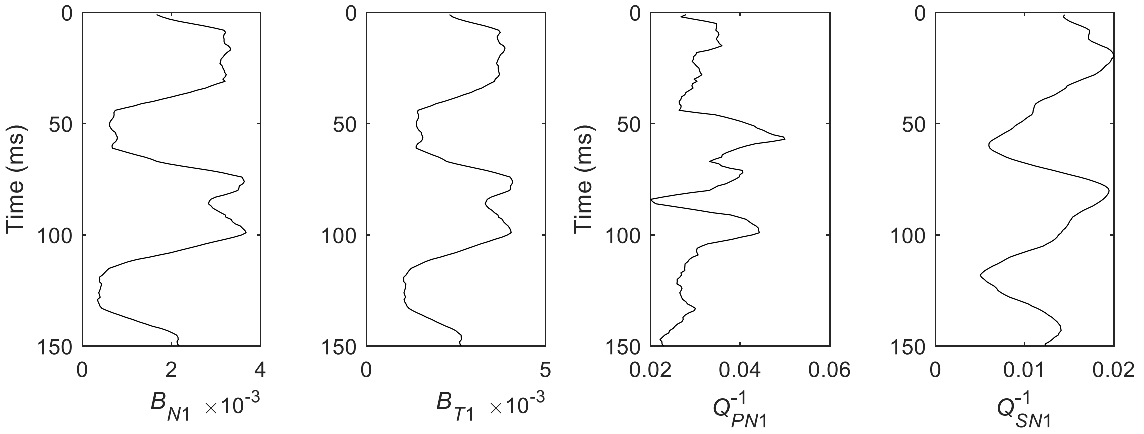

Fig. 2. The curves of specific compliances and integrated attenuative factors constructed as model parameters.

We construct the parameter curves (Fig. 3) of background medium, in which elastic properties V_p, V_s, ρ are taken as known information to compute the reflectivity $R_{PP}^{iso}(\theta), R_{PP}^{adi}(\theta)$, and sensitivity matrix **G** and **S**. WA parameters, specific compliances and integrated attenuative factors curves are taken as model parameters to be solved.

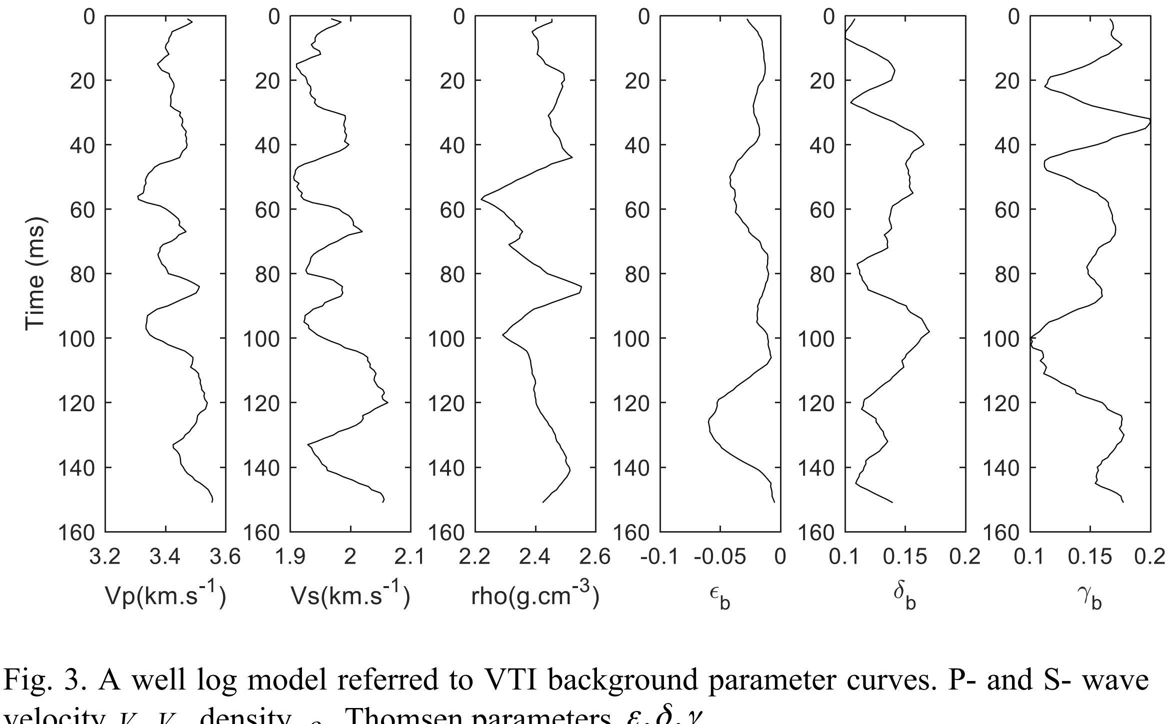

Fig. 3. A well log model referred to VTI background parameter curves. P- and S- wave velocity V_p, V_s, density ρ, Thomsen parameters $\varepsilon, \delta, \gamma$.

Based on convolution theory, we use eq. (16) to synthesize multi-azimuth gathers (Fig. 4a) as the input of inversion. During convolution, a stationary 30 Hz Ricker wavelet are used to smooth reflectivity. In order to trial the stability and accuracy of proposed inversion in noisy environment, we add Gaussian random noise with signal-to-noise ratio (SNR) of 5 and 2 to Fig. 4a, as shown in Figs. 4b and 4c.

a)

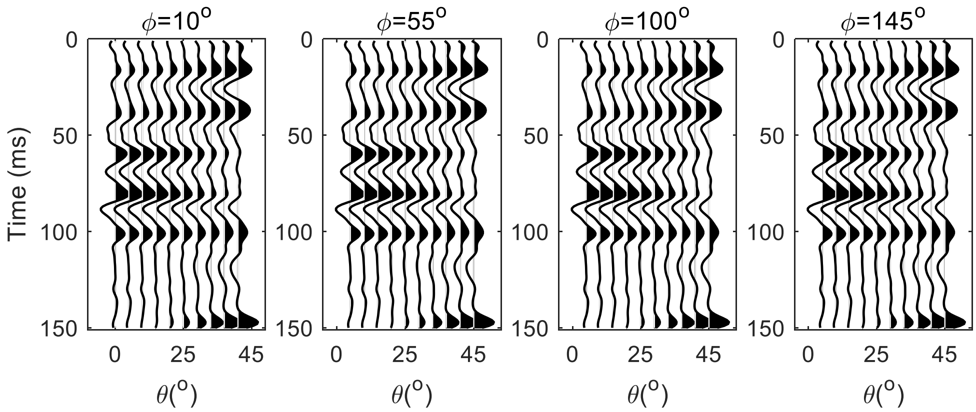

b)

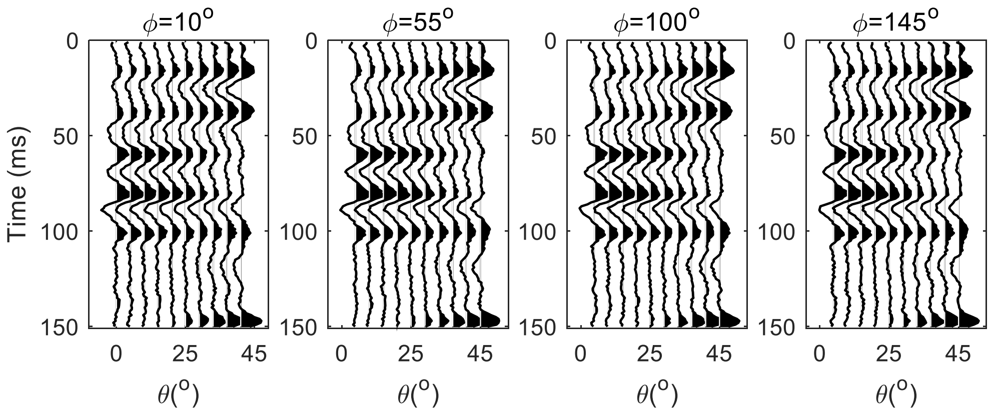

c)

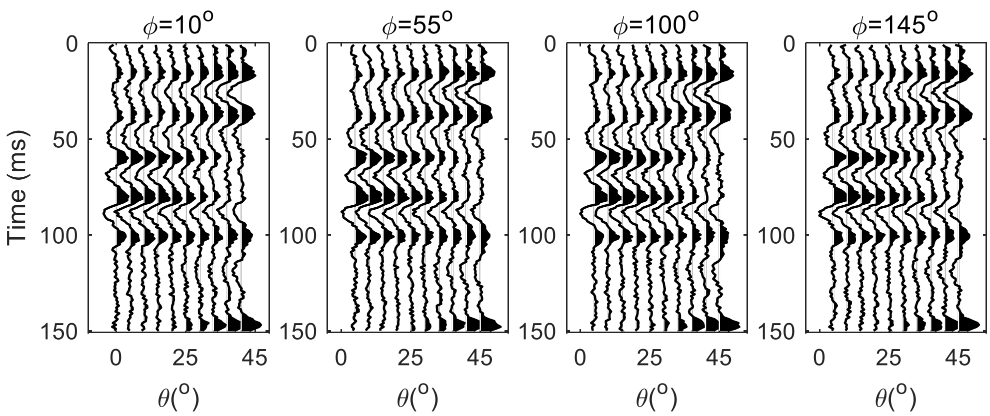

Fig. 4. Synthetic multi-azimuth gathers calculated with the proposed algorithm. (a) noise-free, (b) SNR = 5 and (c) SNR = 2.

We first use the data along fracture strike $\varphi=\phi=70^{o}$ to calculate the WA parameters of VTI background. The corresponding inversion results are displayed in Fig. 5, from which we can observe that stability and accuracy of WA parameters decreases with the increase of noise, but results are in good agreement with the true values.

a)

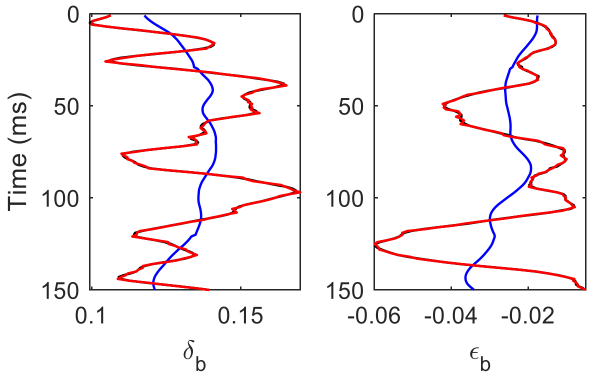

b)

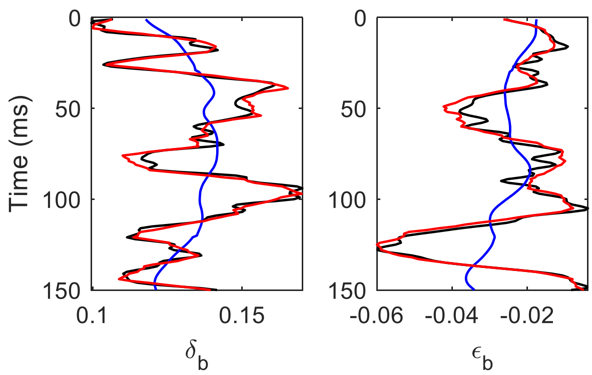

c)

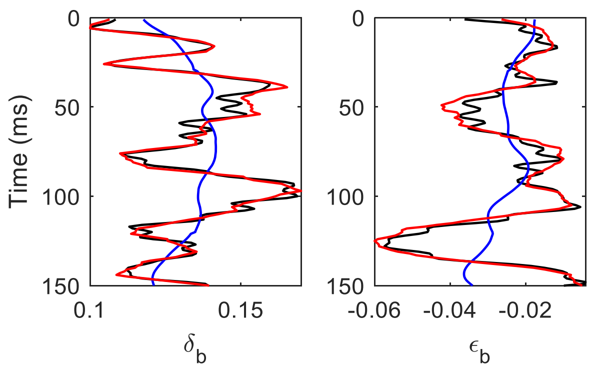

Fig. 5. Comparisons between true values (red) and inversion results (black) of Thomsen parameters. Blue lines mean initial models created by smoothing true values. (a) noise-free, (b) SNR = 5 and (c) SNR = 2.

We next use the obtained VTI background WA parameters as known parameters to perform the second step inversion of specific compliances and integrated attenuative factors. The corresponding inversion results are displayed in Fig. 6. We can observe that stability and accuracy of the four model parameters decreases with the increase of noise. In general, the results can reflect the change trend of truth value.

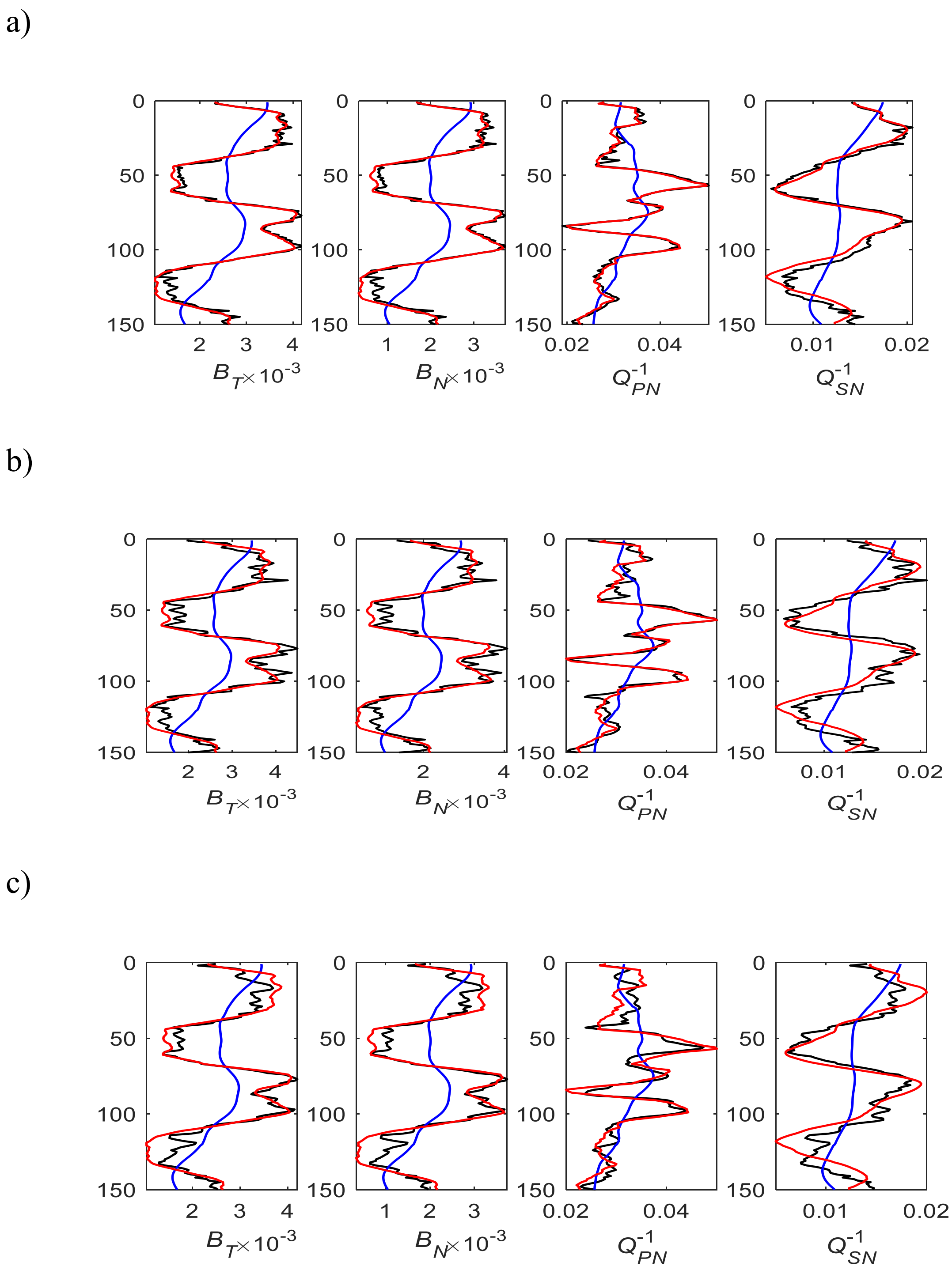

Fig. 6. Comparisons between true values (red) and inversion results (black) of specific compliances and integrated attenuative factors. Blue lines mean initial models created by smoothing true values. (a) noise-free, (b) SNR = 5 and (c) SNR = 2.

DISCUSSION and CONCLUSIONS

Based on frequency-dependent attenuative theory, a two-step linear Bayes' AVOA inversion method for Thomsen parameters, specific compliances and integrated attenuative factors is established for viscoelastic OA media. The application results of synthetic azimuthal gathers reveal that the novel method is reliable in estimation of WA parameters of VTI background, specific compliances and integrated attenuative factors. In proposed method, elastic properties of VTI background in MA media are assumed to be known, and a two-step strategy is suggested in practical inversion. Fracture density, radius and aperture are key characteristic parameters in inversion, which are taken as prior information. It is not realistic to measure the fracture density, radius and aperture of the whole fractured reservoir. It is reasonable to derive the average value of a certain reservoir section according to the survey data or empirical formula of petrophysics researchers. The reliability of the proposed method in estimation of attenuation-related knowledge have been confirmed by using synthetic data.

ACKNOWLEDGEMENTS

We are grateful for the financial support of the following institutions: Science and Technology Cooperation Project of the CNPC-SWPU Innovation Alliance (2020CX020000) and Open Projects Fund of the State Key Laboratory of Oil and Gas Reservoir Geology and Exploitation (PLN201733), National Natural Science Foundation of China (NSFC 41204101).

REFERENCES

Aki, K. and Richards, P.G., 2002. Quantitative Seismology. University Science Books, New York.

Bakulin, A., Grechka, V. and Tsvankin, I., 2000. Estimation of fracture parameters from reflection seismic data. Part I: HTI model due to a single fracture set. Geophysics, 65: 1788-1802.

Biot, M.A., 1962. Generalized theory of acoustic propagation in porous dissipative media. J. Acoust. Soc. Am., 34: 1254-1264.

Buland, A. and Omre, H., 2003. Bayesian linearized AVO inversion. Geophysics, 68: 185-198.

Chen, H. and Innanen, K.A., 2018. Estimation of fracture weaknesses and integrated attenuation factors from azimuthal variations in seismic amplitudes. Geophysics, 83: 1-65.

Chen, H., Innanen, K.A. and Chen, T., 2018. Estimating P- and S-wave inverse quality factors from observed seismic data using an attenuative elastic impedance. Geophysics, 83**(ISSUE No. ???):** R173-R187.

Chapman, M., 2003. Frequency-dependent anisotropy due to meso-scale fractures in the presence of equant porosity. Geophys. Prosp., 51: 369-379.

Chapman, M., Liu, E. and Li, X.Y., 2006. The influence of fluid sensitive dispersion and attenuation on AVO analysis, Geophys. J. Internat., 167: 89-105.

Chapman, M., Zatsepin, S.V. and Crampin, S., 2002. Derivation of a microstructural poroelastic model, Geophys. J. Internat., 151: 427-451.

Chichinina, T., Sabinin, V. and Ronquillo-Jarillo, G., 2006. QVOA analysis: P-wave attenuation anisotropy for fracture characterization, Geophysics, 71**(ISSUE No. ???)**, C37-C48.

Dvorkin, J. and Mavko, G., 2006. Modeling attenuation in reservoir and nonreservoir rock. The Leading Edge, 25: 194-197.

Dvorkin, J., Mavko, G. and Nur, A., 1995. Squirt flow in fully saturated rocks, Geophysics, 60: 97-107.

Dvorkin, J. and Nur, A., 1993. Dynamic poroelasticity: A unified model with the squirt and the Biot mechanisms. Geophysics, 58: 524-533.

Far, M.E., Sayers, C.M., Thomsen, L., Han, D. and Castagna, J.P., 2013. Seismic characterization of naturally fractured reservoirs using amplitude versus offset and azimuth analysis. Geophys. Prosp., 61: 427-447.

Ge, Z.J., Li, J.Y., Chen, X.H., Wu, J.L. and Yu, X., 2018. Bayesian linearized AVAZ inversion for fracture weakness parameters in TTI medium. Chin. J. Geophys., 61: 3008-3018 (in Chinese).

Ge, Z.J., Pan, S.L. and Li, J.Y., 2020. Seismic AVOA inversion for weak anisotropy parameters and fracture density in a monoclinic medium, Appl. Sci., 10: 5136.

Hill, R., 1963. Elastic properties of reinforced solids: Some theoretical principles. J. Mechan. Phys. Solids, 11: 357-372.

Hsu, C.J. and Schoenberg, M., 1993. Elastic waves through a simulated fractured medium. Geophysics, 58: 964-977.

Hudson, J., Liu, E. and Crampin, S., 1996. The mechanical properties of materials with interconnected cracks and pores. Geophys. J. Internat., 124: 105-112.

Mavko, G., Mukerji, T. and Dvorkin, J., 2009. The Rock Physics Handbook: Tools for Seismic Analysis of Porous Media (2nd ed.). Cambridge University Press, Cambridge.

Moradi, S. and Innanen, K.A., 2017. Born scattering and inversion sensitivities in viscoelastic transversely isotropic media. Geophys. J. Internat., 211: 1177-1188.

Pan, S. L., Yan, K., Lan, H.Q. and Qin, Z.Y., 2019. A Bregman adaptive sparse-spike deconvolution method in the frequency domain, Appl. Geophys., 16: 463-472.

Pan, S.L., Yan, K., Lan, H.Q., Badal J. and Qin, Z.Y., 2020a, Adaptive step-size fast iterative shrinkage-thresholding algorithm and sparse-spike deconvolution. Comput. Geosci., 134: 104343.

Pan, S.L., Yan, K., Lan, H.Q., Badal, J. and Qin, Z.Y., 2020b. A sparse spike deconvolution algorithm based on a recurrent neural network and the iterative shrinkage-thresholding algorithm. Energies, 13: 3074.

Pointer, T., Liu, E. and Hudson, J.A., 2000. Seismic wave propagation in cracked porous media. Geophys. J. Internat., 142: 199-231.

Pšencík, I. and Martins, J.L., 2001. Properties of weak contrast PP reflection/transmission coefficients for weakly anisotropic elastic media. Studia Geophys. Geodaet., 45: 176-199.

Sayers, C.M., 2009. Seismic characterization of reservoirs containing multiple fracture sets. Geophys. Prosp., 57: 187-192.

Sayers, C.M. and Kachanov, M., 1995. Microcrack-induced elastic wave anisotropy of brittle rocks. J. Geophys. Res., 100: 4149-4156.

Schoenberg, M. and Sayers, C.M., 1995. Seismic anisotropy of fractured rock. Geophysics, 60: 204-211.

Worthington, M.H., 2008. Interpreting seismic anisotropy in fractured reservoirs. First Break, 26: 57-63.

Zhu, Y. and Tsvankin, I., 2006. Plane-wave propagation in attenuative transversely isotropic media. Geophysics, 71**(ISSUE No. ???)**: T17-T30.